Aerothermodynamics of Sprint-Type Manned Mars Missions

Chul Park*
NASA Ames Research Center, Moffett Field, California 94035
and
Carol B. Davies†
Sterling Software, Palo Alto, California 94303

The aerothermodynamic problems associated with the aerobraking of the spacecraft proposed for the sprint-type fast manned Mars mission are studied. The propulsive ΔV necessary at departure from Earth and Mars and the velocities of the atmospheric entries into the two planets are first deduced from the existing literature by imposing the constraints that the mission be completed within 330 or 436 days. It is shown that entry velocities up to about 15 km/s are possible at both Earth and Mars. Through the trajectory calculations of the vehicles during the aerobraking maneuvers, the requirements on the lift-to-drag ratios (L/D) of the vehicles are deduced under the constraint on the allowed deceleration. L/D values of 0.4 and 1.0 are found to be necessary at Earth and Mars, respectively. Density, pressure, and stagnation-point convective heat-transfer rates are calculated for the typical aerobraking flights. Assuming the shock layer flow to be in equilibrium and the gas to be optically thin for the wavelengths longer than 250 nm and optically thick for the shorter wavelengths, the stagnation-point radiative heat-transfer rates are calculated and shown to be larger than the convective heat-transfer rates.

Nomenclature

L/D = lift-to-drag ratio
P = pressure, atm
q_c = convective heat-transfer rate, W/cm^2 or kW/m^2
q_r = radiative heat-transfer rate, W/cm^2 or kW/m^2
R = nose radius, m
V_{ent} = planetary entry velocity, m/s or km/s
ΔV = velocity change by rocket propulsion, m/s or km/s
ρ = ambient density, g/cm^3 or kg/m^3

Introduction

BECAUSE of the recent worldwide advances in the technology of large launch vehicles and the planned construction of space stations of various sizes by several nations, it has become possible to contemplate a manned mission to the planet Mars in the near future.[1,2] The orbital parameters, that is, the initial and final heliocentric velocities and the transit times, for the trips between Earth and Mars have been calculated in Refs. 3-5. The mission trajectories that minimize the amount of fuel required, that is, the Hohmann transfer orbits, require a total mission time of almost 3 years. Nearly half of the total mission time is the time for layover at Mars while waiting for Mars and Earth to align favorably for the return journey. The point of conjunction (Mars at the far side of the sun from Earth) occurs at the midpoint of the Mars layover; such a mission is called a conjunction mission. The long mission duration for the conjunction mission makes it undesirable for a manned mission because of the possibility that physiological and psychological difficulties with the crew may develop. For a manned mission, it is desirable to reduce the mission time to as small a duration as reasonably possible.

By increasing the velocity of the vehicle at departure, the duration of a one-way trip between any two planets can be shortened. If the Earth-departure velocity is increased beyond a certain critical value so that the vehicle can reach Mars before Earth reaches the point of closest distance, then the trip duration can be shortened drastically. This is because not only the transfer time but the layover time can be shortened. An opposition (Mars and Earth on the same side of the sun) occurs at the midpoint of the mission; such a mission is called an opposition mission.[1] In particular, a mission with a very short travel time is called a sprint mission. The orbital parameters are calculated in Ref. 5 over a range of opposition missions, including sprint missions, occurring between 1965 and 1999. Reference 6 illustrates the merits of such missions in further detail.

Since the opposition-type missions require high orbital speeds between the two planets, the speeds of the vehicles on arrival at the destination planets are correspondingly high. If the vehicles are to be decelerated at the destination planet by the application of rocket thrust (that is, by a retro-burn), the fuel mass required for this purpose would be many times more than the dry mass of the vehicle and would become an additional burden at launch. This fuel requirement can be eliminated by employing aerobraking, that is, utilizing the drag of the vehicle to slow down while flying through the atmosphere, in place of the retro-burn.[1,2]

Thus, one critical element of the technology for the opposition-type manned Mars mission concerns aerobraking of the vehicles in the atmosphere of the two planets. The aerothermodynamic environments of the opposition-type missions have been studied in a cursory fashion in Ref. 1. Reference 2 reviews in somewhat more detail the past studies of the opposition-type missions in which the required high travel speed between the two planets is reduced by swinging by the planet Venus.

The purpose of the present study is to define the aerothermodynamic environments of the aerobraking vehicles for the missions in which the overall mission duration is shorter than in such Venus-swing-by missions. Two mission durations are studied: 330 and 436 days. The 330-day case is chosen because a Soviet cosmonaut has endured approximately this length of time in weightlessness in Earth orbit. The calculations will show that this case requires a very large Earth-departure mass. A 436-day case is chosen arbitrarily and is considered as a

Presented as Paper 89-0313 at the AIAA 27th Aerospace Sciences Meeting, Reno, NV, Jan. 9-12, 1989; received March 2, 1989; revision received March 29, 1990.

*Research Scientist. Associate Fellow AIAA.
†Consultant.

compromise to lower the departure mass. For the purpose of this study of the aerothermodynamic environments, calculations are made for two possible entry velocities at each planet: 12 and 15 km/s at Mars and 14 and 16 km/s at Earth. The reasons for the choice of these entry velocities will be explained later.

The orbital parameter study leads to the belief that, in order to minimize the overall cost of the mission, a manned vehicle must be preceded by an unmanned vehicle that transports the fuel for the return (Mars-to-Earth) journey and for the vehicle to land on Mars. The unmanned cargo vehicle can use the minimum energy orbit, i.e., a conjunction-type orbit, to reach Mars. The combination of the unmanned conjunction mission for the advance cargo vehicle and the sprint mission for the manned vehicle is known as a split-sprint mission. This unmanned advance vehicle can employ aerobraking in the Martian atmosphere in order to reduce the departure mass. Thus the aerothermodynamics of the aerobraking of the unmanned advance vehicle must also be included in an overall study.

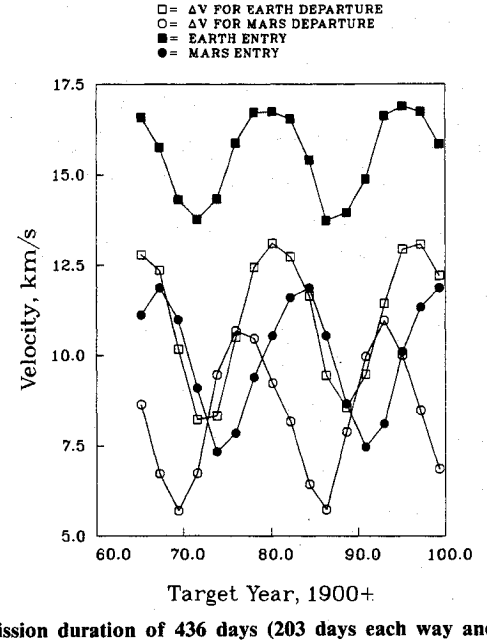

a) Mission duration of 436 days (203 days each way and 30-day Martian layover)

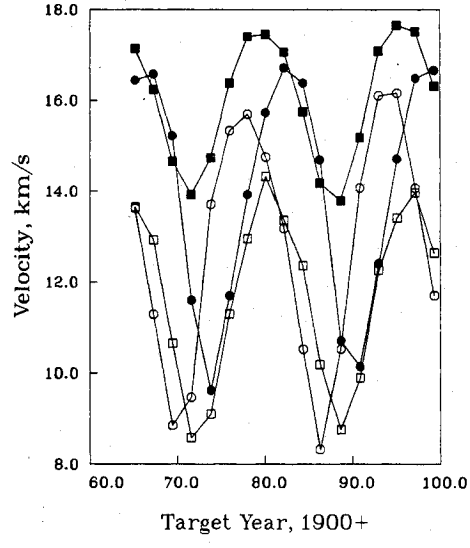

b) Mission duration of 330 days (150 days each way and 30-day Martian layover)

Fig. 1 The propulsive ΔV and entry velocities for a symmetric mission (opposition occurring at the mid-point of the on-Mars activity) to occur between 1965 and 1999, for a fixed mission duration, derived from NASA SP-35 (1963).

For the maximum possible entry velocities, the magnitudes of the lift-to-drag ratio (L/D) required of the aerobraking vehicle are next determined. The trajectory calculations are performed for the aerobraking flights at both Mars and Earth. The environmental parameters (density, pressure, deceleration, and heat-transfer rates) are calculated for various L/D values. The ballistic coefficient is assumed to be 400 kg/m^2 for all these calculations, the justification for which is given later. The calculations show that all environmental parameters are within the range compatible with present or future technology.

Orbital and Mission Parameters

The parameter ΔV and the entry velocity V_{ent} at the two planets are given in Ref. 5 for the sprint-type transfer orbits in charts and tables for the opposition dates falling between 1965 and 1999. The ΔV and entry velocities for the two mission durations of 436 and 330 days, obtained from Ref. 5, are shown in Figs. 1a and 1b for the case of 30-day Mars layover (arrival 15 days prior to opposition and departure 15 days after opposition). The abscissa in these figures are the opposition dates that coincide with the midpoint of the on-Mars activity. The total V_{ent} (i.e., the sum of Mars and Earth entry velocities given in Fig. 1) are plotted in the upper figure in Fig. 2 for the two mission durations. The total departure masses at Earth are estimated using the simplifying assumptions given in Ref. 6 and are shown in the lower figure in Fig. 2. As these figures show, the optimum windows occur at an interval of approximately 17 years, with each window containing two opportunities separated by about 2 years. Extrapolating from the data given in Ref. 2, one expects similar windows to occur in the following years and months prior to 2050: 1) June 2001 and August 2003, 2) October 2020 and December 2022, and 3) November 2037 and December 2039. For the purpose of defining the aerothermodynamic environments, we can assume that these future windows will entail approximately the same conditions as those shown in Figs. 1 and 2.

It can be seen from Figs. 1a and 1b that the entry velocity at Mars varies for these windows from 8.7 to 11 km/s for the 436-day mission and from 10.8 to 15.2 km/s for the 330-day mission. The entry velocity at Earth varies from 13.7 to 14.3 km/s for the 436-day mission and from 13.8 to 14.7 km/s for the 330-day mission for the symmetric case. These led to the choice of the entry velocities of 12 and 15 km/s at Mars and 14 and 16 km/s at Earth.

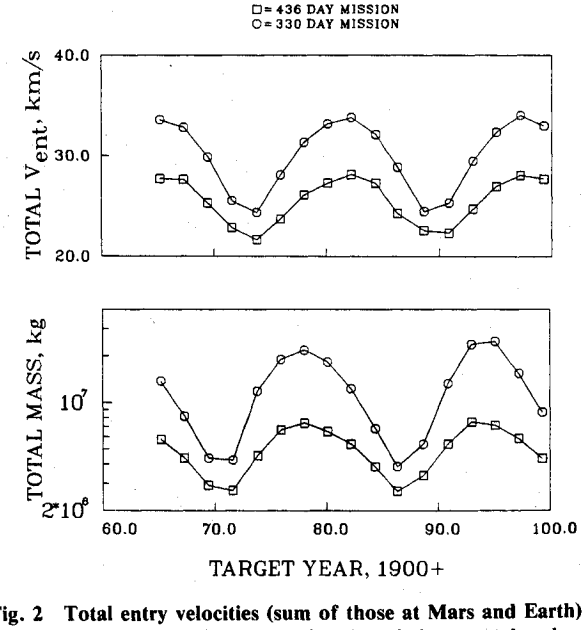

Fig. 2 Total entry velocities (sum of those at Mars and Earth) and the total Earth departure masses for the missions to take place between 1965 and 1999 calculated from NASA SP-35 (1963) under the assumptions described in Ref. 6.

Entry Flight Environments

The trajectories of the aerobraking entry flights of the vehicles in Mars and Earth are calculated to determine the aerothermodynamic environments of these vehicles. The vehicles are assumed to have a ballistic coefficient of 400 kg/m^2, which is approximately half that for the Apollo command module and twice that for the Space Shuttle Orbiter. This value is chosen because the aerodynamic requirements for the vehicles for the manned Mars mission are estimated to fall roughly halfway between those of the Apollo and the Space Shuttle vehicles, The density distribution in the Martian atmosphere is taken from Refs. 7 and 8. The convective heat-transfer rates to the stagnation point of a spherical nose of 3-m radius are calculated for both cases, assuming a fully catalytic wall using the formula of Fay and Riddell.[9] The nose radius of 3 m is similar to that for Apollo. The transport properties in the shock layer in the Martian atmosphere are assumed to be the same as in the Earth's atmosphere for this calculation. The radiative heat-transfer rates are calculated assuming thermochemical equilibrium and optical thinness using the technique to be described in the following section. The reasons for the assumptions will be given there also.

In an aerobraking flight, the flight trajectory must be controlled accurately in order to attain the required postaerobraking apogee. In order to compensate for the possible errors in the entry angle and to navigate through a temporally and spatially varying atmosphere of a planet, the vehicle must execute maneuvers by employing its lift. This can be done either through roll modulation, if the L/D of the vehicle is fixed, or by changing the L/D by deflecting the control surfaces, if the vehicle has such control surfaces. The true vectorial L/D will thus vary throughout the flight. The successful aerobraking flight trajectory achievable using the maximum positive (lift up) L/D of the vehicle in a standard atmosphere is known as the undershoot boundary, whereas that achievable by a maximum negative (lift down) L/D is called the overshoot boundary. The space between these two trajectories is known as the entry corridor, and any successful flight trajectory must lie within the corridor. For the purpose of determining the aerothermodynamic environment, we select a trajectory within the entry corridor, assuming that the vehicle flies at a fixed L/D smaller in magnitude than the vehicle's intrinsic or deployable maximum L/D corresponding to the overshoot and undershoot boundaries. The L/D value chosen can be interpreted to be a time-average of the vectorially varying L/D value of the vehicle. The entry corridor is not calculated because it is immaterial for the purpose of the present study. The time- or flight-averaged L/D value is varied between -0.2 and -1.5 in the calculations.

Figures 3a–3c show a typical time history of the aerothermodynamic parameters during an aerobraking entry flight into the Martian atmosphere with assumed entry velocities of 12 and 15 km/s. Figures 4a–4c show the same parameters for the entry flight into the Earth's atmosphere with assumed entry velocities of 14 and 16 km/s. A flight L/D value of -1.0 was used for the Mars entry and -0.5 for the Earth entry for these examples. The results show that for all cases calculated, the ambient density is of the order of 10^{-7} g/cm^3 at the perigee. The stagnation point pressure is of the order of 0.2–0.4 atm. The peak deceleration (g-load) is in the range of several g, which could possibly be tolerated by the astronauts, provided either 1) the trip duration is quite short, such as in the 330-day mission; or 2) a centrifuge is provided in the vehicle for the astronauts to keep trained in high g. For the Mars entry, the convective heat-transfer rates range from 130 W/cm^2 for the 12-km/s case to 240 W/cm^2 for the 15-km/s case. The range for the Earth entry is from 210 to 320 W/cm^2.

The convective heat-transfer rates shown in Fig. 3c can be extrapolated to cases with different ballistic coefficients through the following reasoning. It is well known that the heat-transfer rate is proportional to $(\rho/R)^{1/2}$ where ρ is the am-

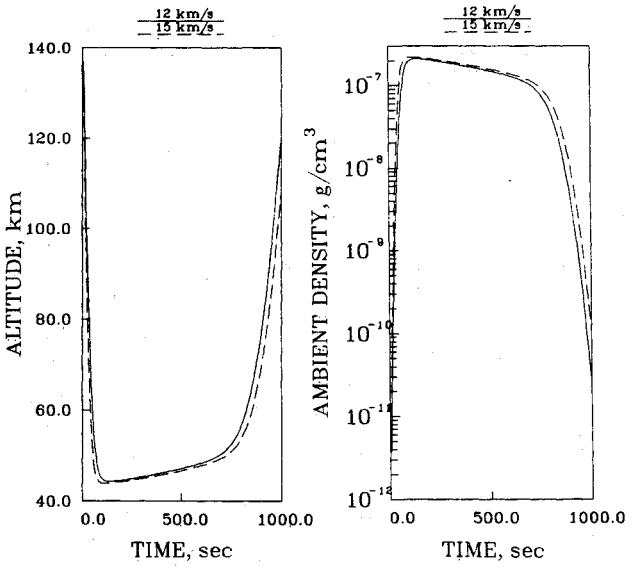

a) Altitude and ambient density

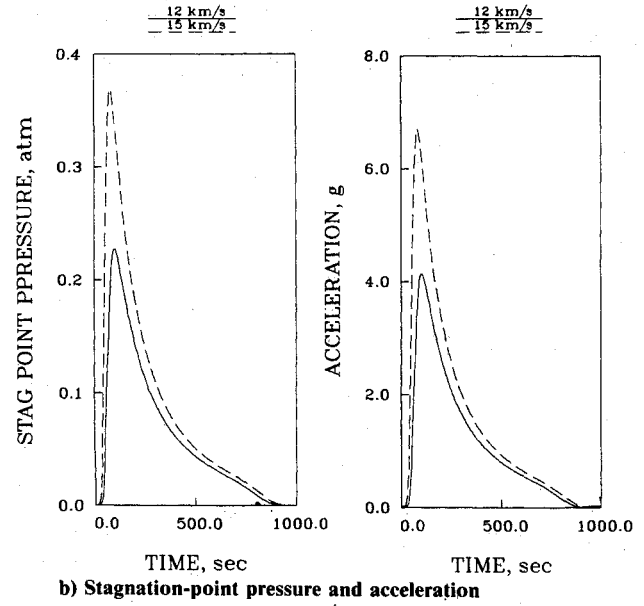

b) Stagnation-point pressure and acceleration

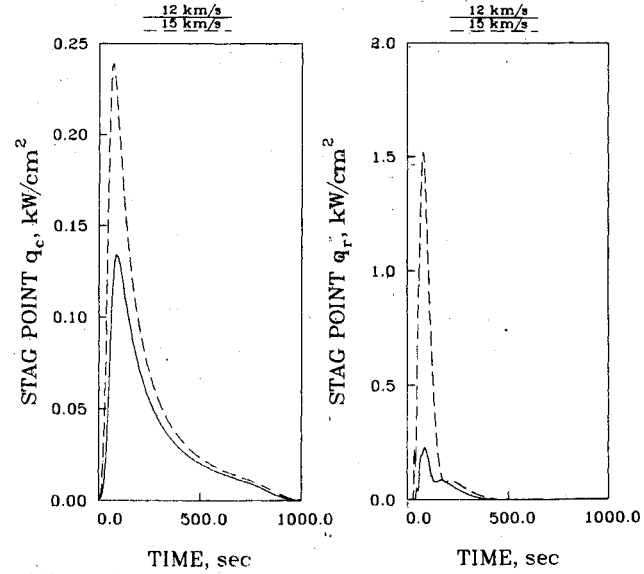

c) Stagnation-point convective and radiative heat-transfer rates q_c and q_r

Fig. 3 Time history of the aerothermodynamic environmental parameters during the aerobraking entry flight in the Martian atmosphere with $L/D = -1$.

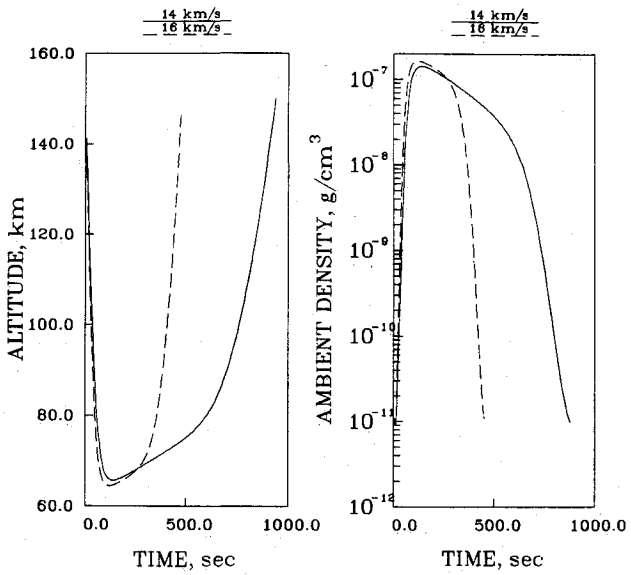

a) Altitude and ambient density

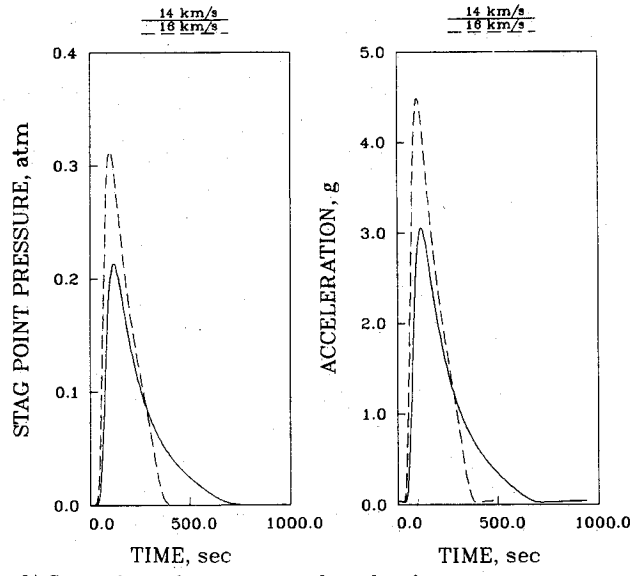

b) Stagnation-point pressure and acceleration

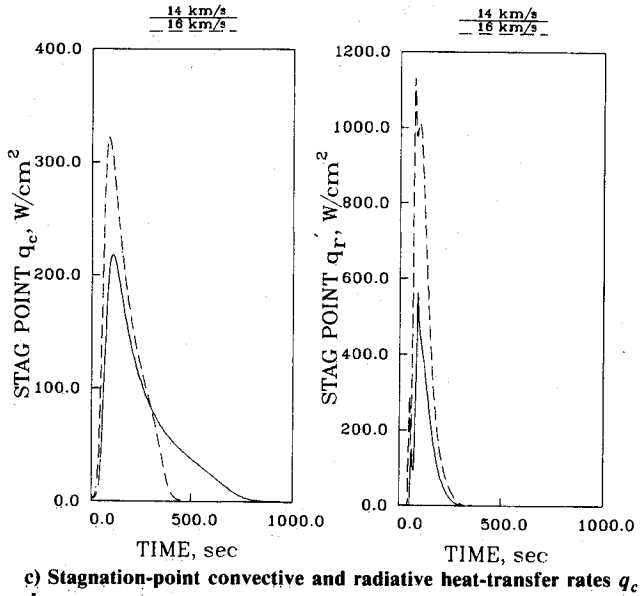

c) Stagnation-point convective and radiative heat-transfer rates q_c and q_r

Fig. 4 Time history of the aerothermodynamic environmental parameters during the aerobraking flights in the Earth's atmosphere with $L/D = -0.5$.

bient atmospheric density and R the characteristic dimension of the vehicle. For a vehicle of a fixed mass and shape, ρ varies linearly with ballistic coefficient,[10] whereas R varies as inverse square root of the ballistic coefficient. Thus the convective heat-transfer rates vary as three-fourth power of the ballistic coefficient. The total (area integrated) heat load is inversely proportional to five-fourth power of the ballistic coefficient.

Also shown in the same figures are the radiative heat-transfer rates, which range from 200 to 1500 W/cm² for the Mars entry and from 600 to 1100 W/cm² for the Earth entry. For the lower entry velocities, the aerothermodynamic environments are comparable to that experienced during the Apollo lunar return mission. For the higher velocities, the total heating rate may approach 2 kW/cm². Although such rates have never been experienced by manned vehicles, they are within the current technology for unmanned systems. In the optically thin approximation used in the present work, radiative heat-transfer rates are proportional roughly to the product ρR, which is, in turn, proportional to a square root of the ballistic coefficient. The maximum g-load for the Earth entry is seen to be less than 4.0 g, likely an acceptable value. However, deceleration at Mars can reach 6.5 g, which is probably intolerable.

The peak g-load is found to be nearly independent of the ballistic coefficient. The peak g-load can be considered to be the ratio between the aerobraking ΔV (the entry velocity minus the exit velocity) and a characteristic deceleration time (typically about 100 s; see Figs. 3b and 4b). In an atmosphere where density varies exponentially with altitude, the deceleration profiles are similar among different flight trajectories generated by different ballistic coefficients. Therefore, the characteristic deceleration time is independent of the ballistic coefficient, and, hence, the peak g-load is independent of the ballistic coefficient.

The impact of changing the (flight-averaged) L/D on the aerothermodynamic environments is shown in Figs. 5a–5d for Martian and Figs. 6a–6d for Earth entry flights. For both Mars and Earth, the maximum convective heat-transfer rates decrease gradually with L/D. For a vehicle of fixed mass, an increase in L/D is achieved partly by a decrease in the drag coefficient and thereby an increase in the ballistic coefficient. Because an increase in ballistic coefficient accompanies an increase in convective heat-transfer rate (see above), the maximum convective heat-transfer rates most likely vary even more gradually with L/D than shown. The convective heat-transfer rates are in the range of several hundred watts per square centimeter, which is of the same order as those for the Apollo vehicles. The heat loads increase substantially with L/D.

In Figs. 5c and 6c, radiative heat-transfer rates for both entries are shown to be up to an order of magnitude higher than the convective heat-transfer rates and the radiative heat loads are about double the convective loads. For the Mars entry, the radiative heat-transfer rates and the total heat load are low and fairly constant for the 12-km/s case. However, for the 15-km/s entry case, the radiative heat-transfer rate is almost 5 kW/cm² at a $-L/D$ of 0.4, dropping rapidly to a value of 1 kW/cm² as $-L/D$ increases to a value of 1.0. The total radiative heat loads also decrease up to a value of $L/D = 1.0$. However, they both remain fairly constant for further increases in $-L/D$, indicating that a $-L/D = 1.0$ would be appropriate for minimizing the heat-transfer rates. At a $-L/D$ of 1.0, the maximum heat loads are of the order of 100 kJ/cm², which is an order of magnitude larger than those for the aeroassisted orbital transfer vehicles[11] and less than half that of the Galileo Probe,[12] which is designed to enter the atmosphere of the planet Jupiter. As shown in Fig. 6d, for the Earth entry, the radiative heat-transfer rates and total heat loads also drop off significantly with increasing $-L/D$, reaching a plateau at a $-L/D$ of about 0.4.

Figures 5b and 6b show the maximum g-load for the Mars and Earth entries for varying L/D. At a $-L/D = 0.4$, the g-load for both entry velocities at Earth are 4 or less, which is

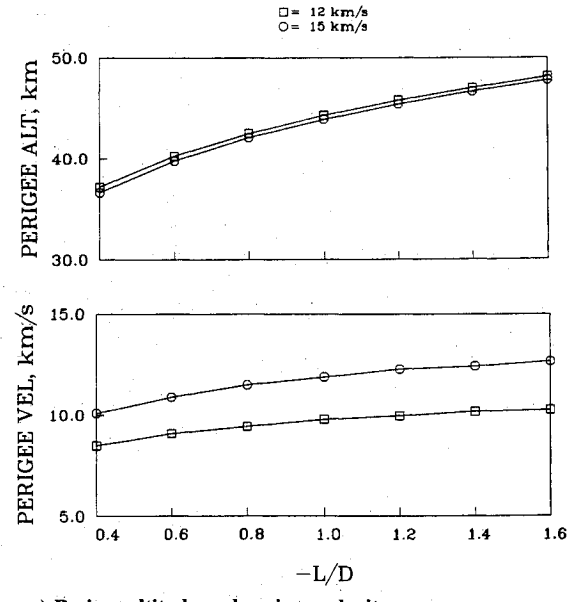

a) Perigee altitude and perigee velocity

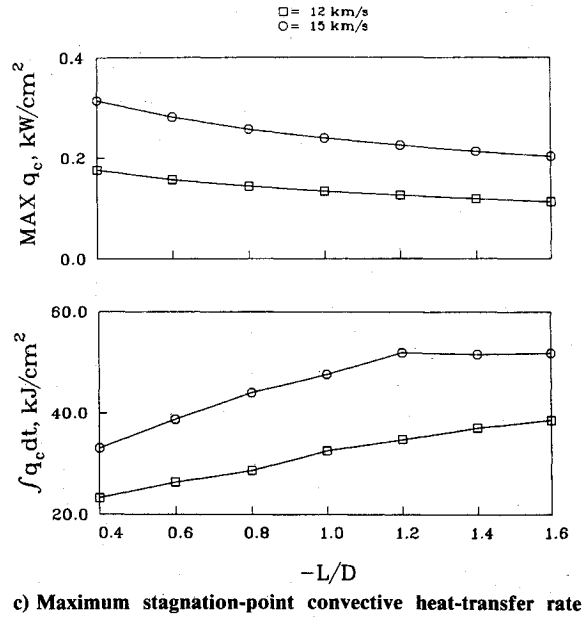

c) Maximum stagnation-point convective heat-transfer rate and convective heat load

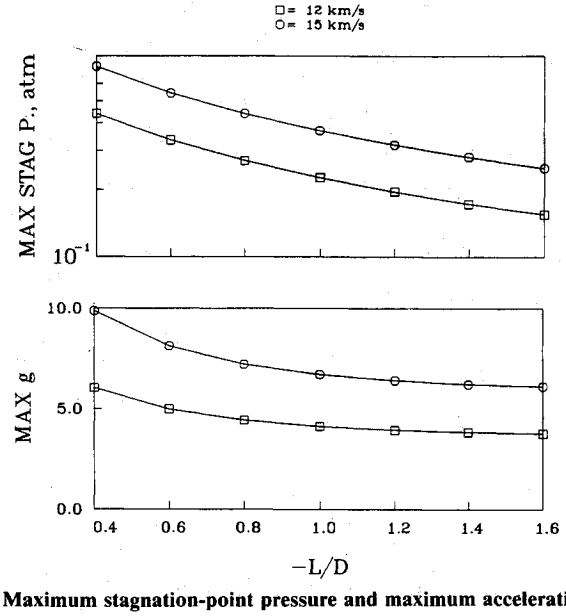

b) Maximum stagnation-point pressure and maximum acceleration

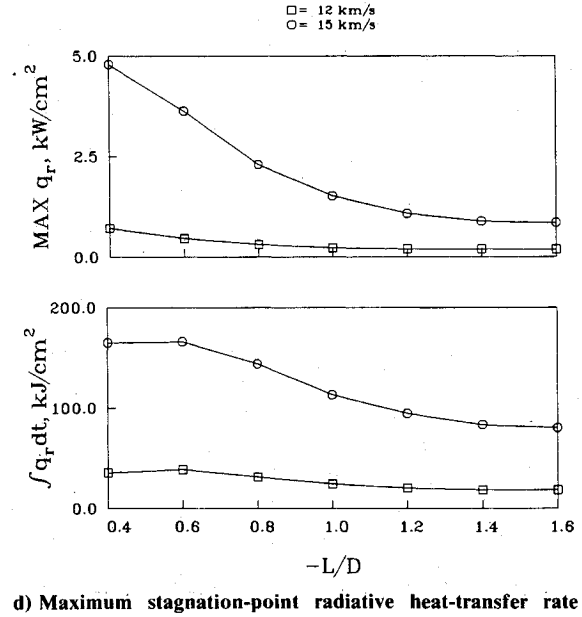

d) Maximum stagnation-point radiative heat-transfer rate and radiative heat load

Fig. 5 The peak environmental parameters in the aerobraking entry flights in the Martian atmosphere as functions of L/D.

likely to be tolerable. However, for the Mars entry, the g-loads are unacceptably high, especially for the 15-km/s entry, ranging from 10 g at a $-L/D$ of 0.4 to 7 g at a $-L/D$ of 1.0. For the lower entry velocity of 12 km/s, the g-load decreases to 5 at a $-L/D$ of 1.0, a more acceptable value. These results indicate that high $-L/D$ values are necessary to reduce the g-loads during Mars entry.

As seen here, one of the most critical quantities seems to be the maximum g-load in the Martian atmosphere. To explore this problem further, calculations are performed for the Martian entry flights over a wider range of entry velocities. The results are shown in Fig. 7. The figure shows that the g-load varies almost linearly with the entry velocity. A higher $-L/D$ value reduces the g-load until it reaches a $-L/D$ value of about 1.0. Increasing $-L/D$ beyond 1.0 has minimum effect. Thus, one concludes that a $-L/D$ value of at least 1.0 should be used for the Martian entry when the entry flight velocity exceeds 10 km/s. For lower entry velocities, a lower $-L/D$ value would be permissible. Menees[13] has shown that for an entry velocity of 6.5 km/s, the maximum g-load is acceptable for vehicles with a flight L/D of -0.1.

Radiative Heating

The radiative heat-transfer rates on the re-entry vehicles in Earth's atmosphere have been studied since the Apollo era. Recently, the predictive capability for radiative heat-transfer rates in Earth's atmosphere has been greatly improved in order to aid the design of the aeroassisted orbital transfer vehicles.[14,15] The radiation intensity is known to be higher in the nonequilibrium region immediately behind a shock wave than in the equilibrium region far behind the shock wave by a factor of several.[15] In the domain where the nonequilibrium phenomenon is dominant, the radiative heat-transfer rate to the stagnation point of a blunt body tends to be proportional to the product ρR in the same manner as in an optically thin gas.[15]

Reference 16 shows that, for a spherical nose of 1-m radius at an entry speed of 14.5 km/s and stagnation pressure of 0.3 atm, the nonequilibrium phenomena cause an increase in the radiative heat flux to the wall by a factor of about 2 over the equilibrium value. For a body of 3-m radius under consideration, the ratio of the nonequilibrium to equilibrium heat fluxes will be closer to unity than for a 1-m body. Besides, the

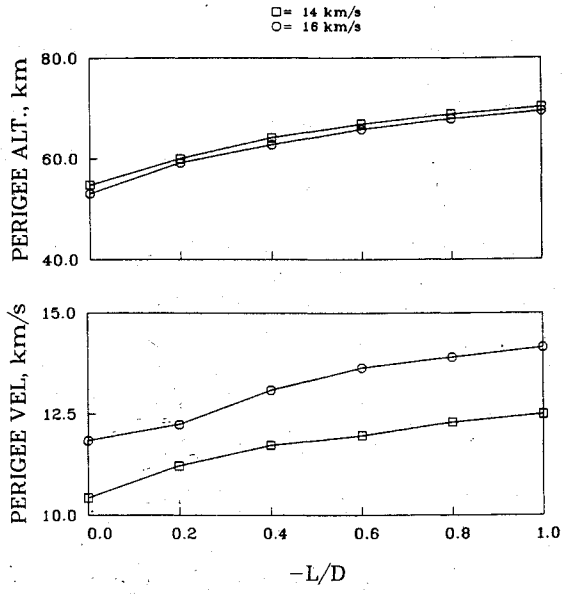

a) Perigee altitude and perigee velocity

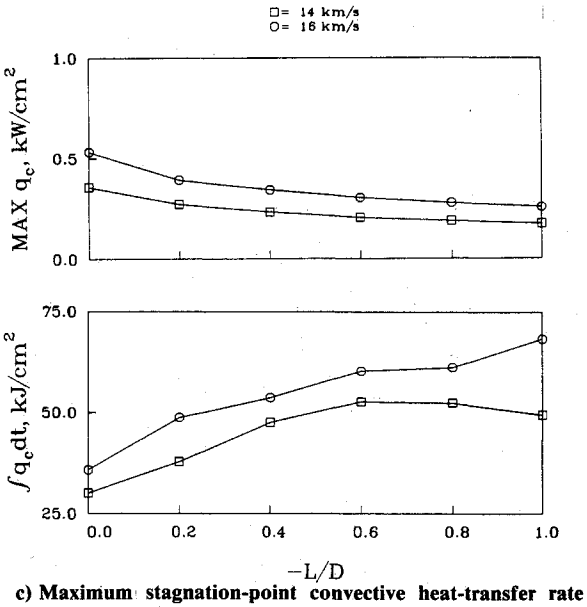

c) Maximum stagnation-point convective heat-transfer rate and heat load

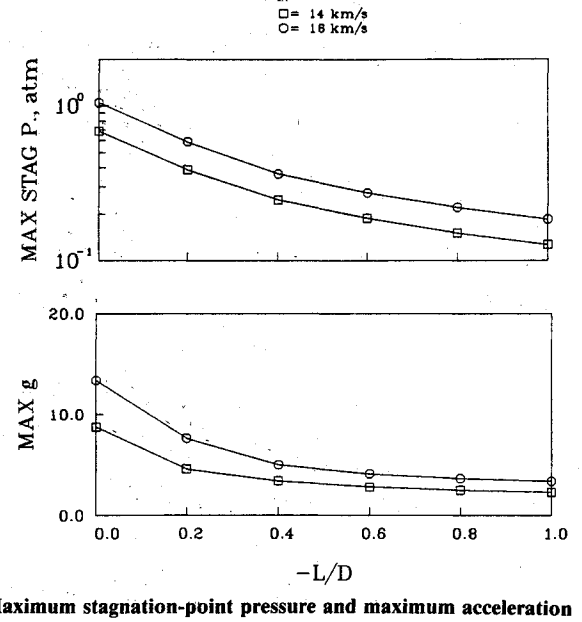

b) Maximum stagnation-point pressure and maximum acceleration

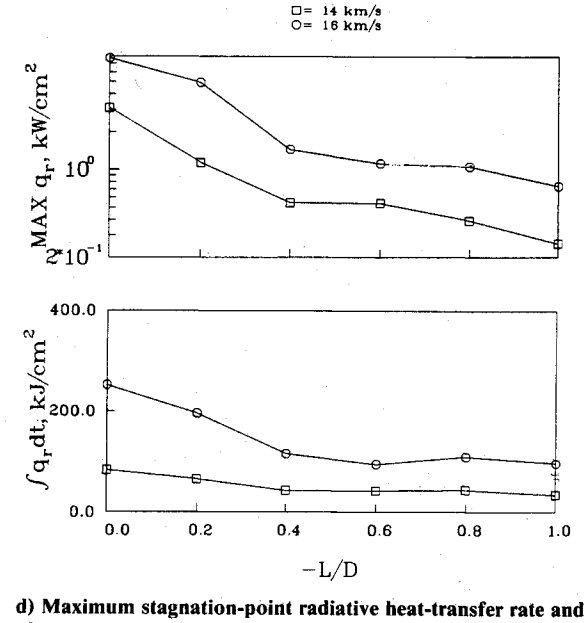

d) Maximum stagnation-point radiative heat-transfer rate and heat load

Fig. 6 The peak environmental parameters in the aerobraking entry flights in Earth's atmosphere as functions of *L/D*.

calculation in Ref. 16 was made without accounting for the radiative cooling of the shock layer. The two phenomena tend to cancel each other, and, as a result, the assumption of equilibrium and optically thin gas yields approximately correct values of radiative heat flux, at least for a body of radius ≥ 3 m flying in air.

In Fig. 8, the radiative emission power per unit volume behind a normal shock wave in air, calculated assuming an equilibrium flow and optically thin gas, is shown as a function of the flight velocity and density. The calculation is made for wavelengths longer than 250 nm and shorter than 3 μm. The radiation in the far ultraviolet wavelength range below 250 nm will probably be absorbed in the ablation layer over the heat shield and, therefore, is not calculated. The calculation was made using the code NEQAIR[14] imposing the equilibrium assumption.

Using the values shown in Fig. 8, the radiative heat-transfer rates to the stagnation point of Earth entry vehicle are calculated for the spherical nose of 3-m radius. The shock layer is assumed to be isothermal and optically thin, and radiative cooling is neglected, for the reason given above. The shock-layer thickness is calculated from the well-known empirical relationship. The results are shown in Figs. 4c and 6d and have been discussed in part already. As the figures show, the absolute values of the rates and heat loads due to radiation are an order of magnitude smaller than those anticipated in the Jovian entry for which heat-shielding technology has already been developed (see, e.g., Ref. 17). However, the time-integrated heat loads are comparable with that for the Jovian entry because of the longer heating period.

Radiative heating rates in the Martian entry flights have also been calculated in the past (e.g., Ref. 18). In Ref. 19, a radiation measurement has been made in a pure CO_2 flow behind a shock wave at a flow velocity between 9 and 12 km/s. The measurement was made in the far-ultraviolet region to observe the radiation from the CO Fourth Positive system. The experiment showed that the CO radiation overshoots in the nonequilibrium region in the same manner as that in air. The times required for equilibration in CO_2 were also determined from the experiment. When these times are compared with those for air, one finds that the equilibration is slower in CO_2 than in air by a factor of several at flow speeds above 10 km/s and by an

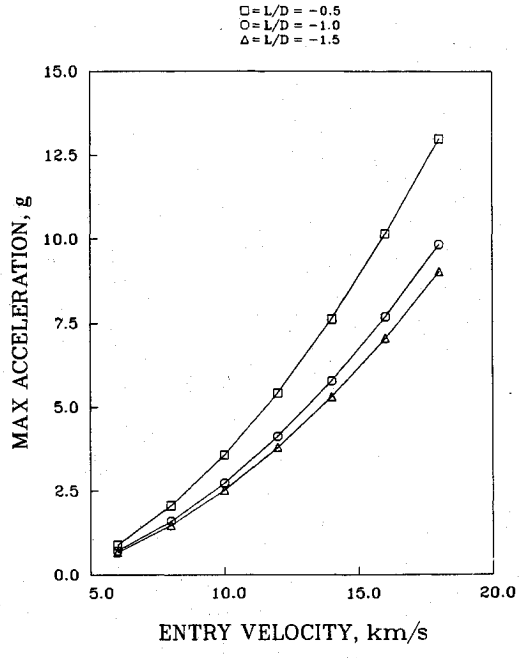

Fig. 7 Maximum acceleration in the Martian atmosphere as a function of entry velocity and *L/D*.

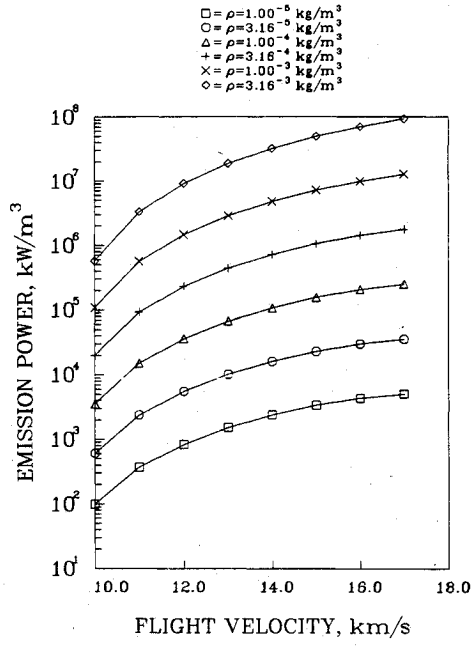

Fig. 8 Radiative power emission in the equilibrium shock layer in the stagnation region in the Earth's atmosphere, for wavelengths longer than 250 mm, as a function of flight velocity and ambient density.

order of magnitude at lower speeds. The equilibration times have been measured also in Ref. 20, which measured the radiation from pure CO_2 in the near-ultraviolet and infrared wavelength regions for (equivalent) flow velocities below 10 km/s. The infrared radiation reached equilibrium much faster than the ultraviolet radiation. The equilibration time for the ultraviolet radiation agreed approximately with that for the far ultraviolet determined in Ref. 19 at the overlapping velocities. Based on the far ultraviolet data of Ref. 19 and the near-ultraviolet data of Ref. 20, the equilibration distance behind the bow shock wave in the Martian atmosphere at a flight speed of 8 km/s and stagnation pressure of 0.3 atm is calculated to be > 30 cm. Interestingly, nonequilibrium overshoot of radiation was observed for the infrared but not for the ultraviolet radiation in the work of Ref. 20. On the other hand, Ref. 21 observed radiation in the violet region in N_2-CO_2 mixtures. A strong nonequilibrium overshoot was seen in the experiment, which was attributed mostly to CN Violet system.

There are many questions still unanswered regarding the nonequilibrium phenomena in Martian atmosphere. However, examination of Refs. 19–21 leads one to the following tentative conclusions:

1) At entry velocities above 12 km/s, the equilibration distance is still a small fraction of the typical shock-layer thickness, and nonequilibrium phenomena cause an increase in radiative heat-transfer rate only to within a factor of 2. This small nonequilibrium enhancement of radiation tends to cancel the radiative cooling phenomena. Therefore, the assumption of an equilibrium flow and optically thin gas is likely to yield approximately correct values of radiative heat fluxes in this high velocity range.

2) At entry velocities below 10 km/s, the equilibration distance becomes a significant fraction of the shock-layer thickness. The overshoot of radiation in the nonequilibrium is very large. In this velocity range, a detailed nonequilibrium calculation is needed to determine the radiative heat-transfer rates. A radiation calculation based on the assumption of equilibrium can be considered to be merely a reference point.

In the present work, the calculations are made assuming equilibrium and optically thinness, using the composition data obtained in the Viking mission,[8] according to which the atmosphere consists of 2.7% N_2, 95.7% CO_2, and 1.6% A (argon). The equilibrium radiations from the CO Fourth Positive system, C_2 Swan system, CN Violet and Red systems, and O_2 Schumann-Runge system are included among the molecular species. Nitrogen radiation is neglected because its concentration is small. Among the atoms, atomic carbon and atomic oxygen are included. The calculation is made only for wavelengths greater than 250 nm because of the belief that the shorter wavelengths will be absorbed in the ablation layer. The results are shown in Fig. 9. Compared with the existing calculations, such as Ref. 18, the present values are slightly lower because of the neglecting of the shorter wavelengths and of the nitrogen radiation.

The radiative heat-transfer rates to the stagnation point are calculated for the Martian entry vehicle with a 3-m nose radius using the values in Fig. 9. The results are shown in Figs. 3c and 5d and also have been discussed in part in the preceding section. The radiative heat-transfer rates and heat loads are comparable to those in the Galileo mission.[12,17]

Further Considerations

The foregoing discussions point to the fact that most of the aerothermodynamic environments are similar to those of Apollo, aeroassisted orbital transfer vehicles, or Galileo Probe vehicle. However, several features unique to the manned Mars mission become apparent. First, the *g*-load problem compels one to choose a high *L/D* configuration, especially for the Martian aerobraking. Developing high *L/D* aerobrakes will require a significant amount of research and development. The radiative heat-transfer problem compels one to choose a relatively small nose radius, smaller than 3 m, for such a massive body. Providing a heat shield suitable for such an environment is an interesting challenge.

The raked-off cone geometries appropriate for an *L/D* of −0.5 have a relatively large base region. The main body of the vehicle, including the fuel tanks, must be placed within this base region in the form of an afterbody. The convective and radiative heating of the afterbody could be significant and so requires study.

The high *L/D* is also desirable in the Martian atmosphere in order to navigate through the uncertain atmosphere of the planet. At the contemplated flight velocities, calculations show that the flight trajectories in the Martian atmosphere are

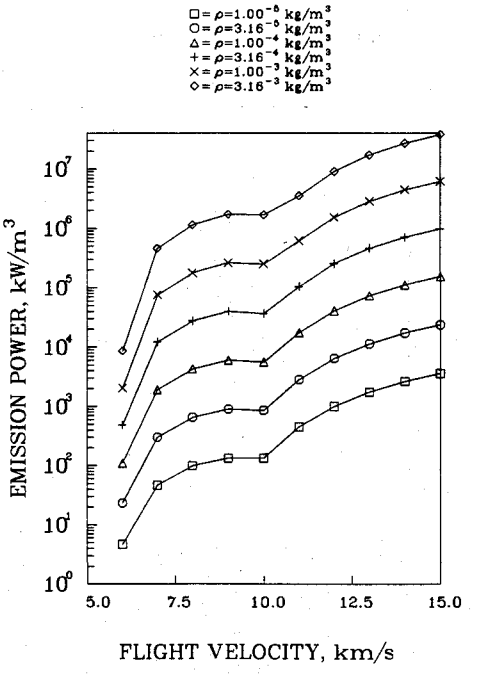

Fig. 9 Radiative power emission in the equilibrium shock layer in the stagnation region in the Martian atmosphere, for wavelengths longer than 250 nm, as a function of flight velocity and ambient density.

very sensitively affected by a small change in the ambient density and the L/D of the vehicle. It is highly desirable to know the trim angle of attack for the Martian aerobraking vehicle beforehand. To do so, the real gas effects on aerodynamic trim must be understood. The pressure distribution in the base or the vehicle leeward side must be determined accurately for this purpose.

One must investigate the extent of radiation enhancement by nonequilibrium. The nonequilibrium radiation problem is especially acute for the Martian entries at speeds below 10 km/s. As mentioned earlier, the equilibrium radiation data for the Martian case in this flight speed range presented in the present work is for reference only.

Conclusions

For the split-sprint-type manned Mars mission:

1) The Mars entry velocities range from 9 to 11 km/s for the 436-day mission and from 11 to 15 km/s for the 330-day mission. The corresponding Earth entry velocities range from 13.7 to 14.3 km/s for the 436-day mission and from 13.8 to 14.7 km/s for the 330-day mission.

2) The g-load is a limiting factor for Mars entry. An entry velocity of 15 km/s for a 330-day mission produces a deceleration greater than 6 g. For a 436-day mission, it is below 4 g.

3) The vehicle must fly such that the time-averaged value of L/D is about -1.0 for the manned Mars entry with a velocity above 12 km/s, and -0.4 for the manned Earth entry with a velocity above 14 km/s.

4) The total heat loads on the aerobrakes at the two planets are several times those for the Apollo vehicle but less than half of those for the Galileo Probe vehicle.

5) Nonequilibrium radiation may be important for the Martian entry at velocities below 10 km/s.

Acknowledgment

The authors wish to express thanks to M. E. Tauber of Ames Research Center for his valuable suggestions and discussions that were incorporated in this paper.

References

[1]NASA and Los Alamos National Laboratories, "Manned Mars Missions: Working Group Papers," Vol. 1, NASA TM-89320, and Vol. 2, NASA TM-89321, June 1988.

[2]Walberg, G. D., "A Review of Aerobraking for Mars Missions," 39th Congress of the International Astronautical Federation, Bangalore, India, Paper 88-196, Oct. 1988.

[3]Sergeyevsky, A. B., Snyder, G. C., and Cunniff, R. A., "Interplanetary Mission Design Handbook, Volume 1, Part 2, Earth-to-Mars Ballistic Mission Opportunities, 1990–2005," Jet Propulsion Lab., Pub. 82-43, Sept. 1983.

[4]Sergeyevsky, A. B., and Cunniff, R. A., "Interplanetary Mission Design Handbook, Volume 1, Part 5, Mars-to-Earth Ballistic Mission Opportunities, 1992-2007," Jet Propulsion Lab., Pub. 82-43, Dec. 1987.

[5]Lockheed Missile and Space Co., "Planetary Flight Handbook," Vol. 3, Pts. 1-3, NASA SP-35, 1963.

[6]Park, C., and Davies, C. B., "Aerothermodynamics of Sprint-Type Manned Mars Mission," AIAA Paper 89-0313, Jan. 1989.

[7]Tauber, M. E., and Yang, L., "The Heating Environment During Martian Atmospheric Descent," AIAA Paper 88-2671, June 1988.

[8]Seiff, A., and Kirk, D. B., "Structure of the Atmosphere of Mars in Summer at Mid-Latitudes," *Journal of Geophysical Research,* Vol. 82, No. 28, 1977, pp. 4364–4378.

[9]Fay, J. A., and Riddell, F. R., "Theory of Stagnation Point Heat Transfer in Dissociated Air," *Journal of the Aeronautical Sciences,* Vol. 25, No. 2, Feb. 1958, pp. 73–97.

[10]Park, C., "A Review of Shock Waves Around Aeroassisted Orbital Transfer Vehicles," NASA TM-86769, June 1985.

[11]Menees, G. P., "Trajectory Analysis of Radiative Heating for Planetary Missions with Aerobraking of Spacecraft," AIAA Paper 83-0407, Jan. 1983.

[12]Sutton, K., Jones, J. J., and Powell, R. W., "Effects of Atmospheric Structure on Radiative Heating for Jupiter Entry Probe," *Progress in Astronautics and Aeronautics: Outer Planet Entry Heating and Thermal Protection,* Vol. 64, edited by R. Viskanta, AIAA, New York, 1979, pp. 3–21.

[13]Menees, G. P., "Aeroassisted-Vehicle Design Studies for a Manned Mars Mission," 38th Congress of International Astronautical Federation, Brighton, UK, Paper 87-433, Oct. 1987.

[14]Park, C., "Calculation of Nonequilibrium Radiation in the Flight Regimes of Aeroassisted Orbital Transfer Vehicles," *Progress in Astronautics and Aeronautics: Thermal Design of Aeroassisted Orbital Transfer Vehicles,* Vol. 96, edited by H. F. Nelson, AIAA, New York, 1985, pp. 395–418.

[15]Park, C., "Assessment of Two-Temperature Kinetic Model for Ionizing Air," *Journal of Thermophysics and Heat Transfer,* Vol. 3, No. 3, 1989, pp. 233–244.

[16]Park, C., and Milos, F. S., "Computational Equations for Radiating and Ablating Shock Layers," AIAA Paper 90-0356, Jan. 1990.

[17]Park, C., Lundell, J. H., Green, M. J., Winovich, W., and Covington, M. A., "Ablation of Carbonaceous Materials in a Hydrogen-Helium Arcjet Flow," *AIAA Journal,* Vol. 22, No. 10, 1984, pp. 1491–1498.

[18]Woodward, H. T., "Predictions of Shock-Layer Radiation from Molecular Band Systems in Proposed Planetary Atmospheres," NASA TN-D-3850, Feb. 1967.

[19]Nealy, J. E., "An Experimental Study of Ultraviolet Radiation Behind Incident Normal Shock Waves in CO_2 at Venusian Entry Speeds," AIAA Paper 75-1150, Sept. 1975.

[20]Davies, W. O., "Carbon Dioxide Dissociation at 6000 to 11,000° K," *Journal of Chemical Physics,* Vol. 43, No. 8, 1965, pp. 2809–2818.

[21]Arnold, J. O., and Nicholls, R. W., "A Shock-Tube Determination of the CN Ground State Dissociation Energy and Electronic Transition Moments for the CN Violet and Red Band Systems," *Proceedings of the 9th International Shock Tube Symposium, 1973,* Stanford University Press, 1974, pp. 340–351.